

Critically fast pick-and-place with suction cups

Hung Pham, Quang-Cuong Pham

Abstract—Fast robotic pick-and-place with suction cups is a crucial component in the current development of automation in logistics (factory lines, e-commerce, etc.) By “critically fast” we mean the fastest possible movements for transporting an object such that it does not slip or fall from the suction cup. The main difficulties are: (i) handling the contact between the suction cup and the object, which fundamentally involves kinodynamic constraints; and (ii) doing so at a low computational cost, typically a few hundreds of milliseconds. To address these difficulties, we propose (a) a model for suction cup contacts, (b) a procedure to identify the contact stability constraint based on that model, and (c) a procedure to parameterize, in a time-optimal manner, arbitrary geometric paths under the identified contact stability constraint. We experimentally validate the proposed pipeline on a physical robot system: the cycle time for a typical pick-and-place task was less than 5 seconds, planning and execution times included. The full pipeline is released as open-source for the robotics community.

I. INTRODUCTION

Suction cups have proved to be some of the most robust and versatile devices to grasp a variety of objects, and are therefore used in a large proportion of automation solutions in logistics (factory lines, e-commerce, etc.) In addition to robustness and versatility, cycle time is another key driver in the development of automation: how fast automated systems can pick and place objects is a decisive economic question.

In this paper, we are interested in planning and executing critically fast pick-and-place movements with suction cups. By “critically fast” we mean the fastest possible movements for transporting an object such that it does not slip or fall from the suction cup. Another major concern is to also minimize the planning time. Indeed, in a majority of e-commerce scenarios, the robot movements must be computed based on the dynamically perceived positions of the objects to be transported, which implies that both planning and execution times contribute to the total cycle time.

Note that, to focus on the planning and execution aspects, we assume in this paper that the perception problem has been solved upstream: (i) a good model of the environment is available, (ii) the geometries, weight distribution, and initial positions/orientations of the objects are given and accurate.

Essentially, ensuring that the object being transported does not slip or fall amounts to guaranteeing that, at every moment, the net inertial wrench acting on the object can be physically “realized” by its contact with the suction cup (weak contact stability [1], [2]). Since inertial wrenches



Fig. 1. Critically fast pick-and-place of a box with a suction cup. The full video of the experiment is available at <https://youtu.be/b9H-zOYWLbY>.

can be easily computed given a sufficiently accurate model of the object, this task is reduced to identifying the set of wrenches that are *physically realizable* for the given suction cup contact. A procedure for doing this is among the contributions of this paper. In the following, we will refer to this objective as satisfying the *suction cup grasp stability constraint*, or simply *grasp stability constraint*.

In industrial robotic pick-and-place systems, a popular approach to maintaining suction cup grasp stability is to uniformly restrict the robot’s joint velocity and acceleration. The velocity and acceleration limits can be tuned by executing multiple test trajectories, then selecting the set of limits at which there is no failure and the average duration is the shortest. A drawback of this approach is that testing must be done for each object/suction cup combination, and therefore, is tedious and time consuming. Furthermore, it is certain that the resulting movements are not optimal, since the kinematic limits are chosen with respect to *all* testing trajectories. Also, there is no guarantee that the robot can successfully execute any new, untested trajectory during its actual operation.

An equally important concern is that the computational cost of planning should be small, as otherwise it would undermine the benefit of controlling the robot to move critically fast. For example, suppose one is capable of computing the true time-optimal trajectories, but requires a few seconds per trajectory. In this case, it might be more reasonable to use a sub-optimal approach that has cheaper computational cost, such as limiting the robot’s joint velocity and acceleration. In the same way, the planning procedure needs to be reliable:

Hung Pham and Quang-Cuong Pham are with Singapore Centre for 3D Printing (SC3DP), School of Mechanical and Aerospace Engineering, Nanyang Technological University, Singapore (email: pham0074@e.ntu.edu.sg, cuong.pham@normalesup.org)

it has to detect infeasible instances correctly, and is robust against numerical errors.

In this paper, we propose an approach for planning critically fast movements for robotic pick-and-place with suction cups. This approach is computationally efficient and robust, and is verified experimentally to be capable of producing near time-optimal movements. This performance is achieved by means of three main technical contributions:

- A model for suction cup contacts (Section II-C);
- A procedure to compute and approximate the contact stability constraint based on that model (Section II-D);
- A procedure to parameterize, in a time-optimal manner, arbitrary geometric paths under the identified contact stability constraint (Section III).

The full pipeline is available as open-source¹. Experimental results are reported and discussed in Section IV. A discussion of related works is postponed to Section V.

II. GRASP STABILITY FOR SUCTION CUPS

A. Background 1: Linearized friction cone

In suction cup grasping, frictional forces exist between the suction cup's pad and the object; these forces are fundamental for maintaining a stable grasp. These frictional forces are modelled using the Colomn friction model. Let $\mathbf{f} = (f_x, f_y, f_z)$ denote a friction force vector, μ denote the coefficient of friction and let the Z-axis be the normal contact direction, the Colomn friction model states

$$\|(f_x, f_y)\|_2 \leq \mu f_z. \quad (1)$$

The set of feasible friction forces, or equivalently the feasible set of inequality (1), is a Second-Order cone² [3] and hence, can be approximated by a polyhedral cone with arbitrary precision [4]. For instance, an approximation with 4 linear inequalities is given as follows:

$$\begin{bmatrix} -1 & -1 & -\mu \\ -1 & 1 & -\mu \\ 1 & 1 & -\mu \\ 1 & -1 & -\mu \end{bmatrix} \begin{bmatrix} f_x \\ f_y \\ f_z \end{bmatrix} \leq \mathbf{0}_4. \quad (2)$$

This approximation is known as the *linearized friction cone*. This is also the approximation we use in this paper.

B. Background 2: Polyhedral computations

A polytope can be defined as the feasible set of a system of linear equalities and inequalities:

$$\mathbf{Ax} \leq \mathbf{b}, \mathbf{Cx} = \mathbf{d},$$

where \mathbf{A} , \mathbf{b} , \mathbf{C} , \mathbf{d} are matrices of suitable dimensions. This representation is known as the H-representation, where H stands for halfspace. Alternatively, a polytope can also be defined as the Minkowski sum³ of the convex hull of a finite

¹<https://github.com/hungpham2511/rapid-transport>

²Also known as a Lorentz cone or an ice-cream cone.

³The Minkowski sum of two sets P, Q is defined as

$$\{x + y \mid x \in P, y \in Q\}$$

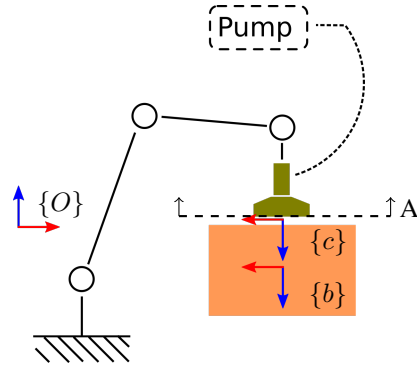


Fig. 2. Diagram of a robotic system for pick-and-place.

number of points and the conic hull of a finite number of rays:

$$\left\{ \sum_i \theta_i \mathbf{u}_i \mid \sum_i \theta_i = 1; \forall i, \theta_i \geq 0 \right\} + \left\{ \sum_i \theta_i \mathbf{v}_i \mid \forall i, \theta_i \geq 0 \right\}.$$

The vertices \mathbf{u}_i (resp. rays \mathbf{v}_i) are referred to as the *generating* vertices (resp. rays). This representation is known as the V-representation, where V stands for vertex.

A seminal result in the theory of polyhedral computation, discovered by Minkowski and Weyl, is that any polytope has both a H-representation and a V-representation [5]. The problem of computing the V-representation given the H-representation is *vertex enumeration*; and the dual problem is *facet enumeration*. Even though both problems are known to be NP-hard, algorithms, such as the Double Description method [5] or the Reversed Search algorithm [6], have been developed to solve them in reasonable times. Both algorithms have publicly available implementations.

C. A model for suction cup grasping

The interface between the suction cup on the object is modelled as consisting of a collection of point forces: one suction force and m contact points⁴ (See Fig. 3). The suction force, denoted by $\mathbf{f}^{(0)}$, satisfies

$$\mathbf{f}_0^{(0)} = [0, 0, PA]^\top, \quad (3)$$

where P is the negative pressure in Pa and A is the area of the suction cup in m^2 . At the i -th contact point, the cup exerts on the object a force $\mathbf{f}^{(i)}$ that follows the linearized Colomn friction model (2). The suction and contact forces $\mathbf{f}^{(i)}, i = 0, \dots, m$ with the corresponding local frames $\{i\}, i = 0, \dots, m$ are depicted in Fig. 3.

The contact wrench exerted on the object by the cup depend on the suction and contact forces. Indeed, let $\{c\}$ denote a frame that is attached rigidly to the suction cup. By transforming all individual forces to frame $\{c\}$ and adding them together, one obtains the net wrench \mathbf{w}_c :

$$\mathbf{w}_c = \sum_{i=0}^m \mathbf{G}_{ci} \mathbf{f}_i^{(i)}, \quad (4)$$

⁴From [2], adopting the point-force formulation does not incur any loss in generality as compared to the surface-force formulation

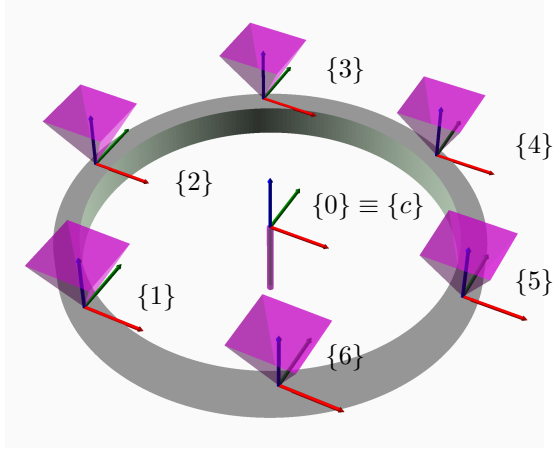


Fig. 3. Cross-sectional view (cross section A in Fig. 2) of the contact between the cup and the object. The physical contact area is modelled by m point forces following the linearized Coulomb friction model and 1 point force capturing the suction force due to negative pressure. A local frame is defined at each point contact.

where the matrix \mathbf{G}_{ci} is defined via the position vector \mathbf{p}_{ci} and rotational matrix \mathbf{R}_{ci} of frame $\{i\}$ in frame $\{c\}$ as below

$$\mathbf{G}_{ci} = \begin{bmatrix} [\mathbf{p}_{ci} \times] \mathbf{R}_{ci} \\ \mathbf{R}_{ci} \end{bmatrix}.$$

We make an assumption concerning the realizability of a contact wrench: a contact wrench \mathbf{w}_c is physically realizable if there exists a set of individual contact forces $\mathbf{f}^{(0)}, \dots, \mathbf{f}^{(m)}$ that satisfies Equation (2) and (3). This condition is often used in humanoid locomotion [7] and is known as the *weak contact stability condition* [1].

The *exact* grasp stability constraint can now be shown to have the form

$$\mathbf{F}_c \mathbf{w}_c \leq \mathbf{g}_c, \quad (5)$$

where \mathbf{F}_c and \mathbf{g}_c are matrices of appropriate sizes. We demonstrate this result by presenting the below constructive procedure:

- 1) let $\hat{\mathcal{F}}$ be the set of feasible values of $\hat{\mathbf{f}} := \{\mathbf{f}^{(0)}, \dots, \mathbf{f}^{(m)}\}$; form the H-representation of $\hat{\mathcal{F}}$;
- 2) compute the corresponding V-representation, which is a set of generating vertices⁵ ($\hat{\mathbf{f}}_1, \dots, \hat{\mathbf{f}}_l$);
- 3) use Equation (4) to transform ($\hat{\mathbf{f}}_1, \dots, \hat{\mathbf{f}}_l$) to ($\hat{\mathbf{w}}_1, \dots, \hat{\mathbf{w}}_l$); \mathcal{W}_c is the convex hull of ($\hat{\mathbf{w}}_1, \dots, \hat{\mathbf{w}}_l$);
- 4) compute the H-representation of \mathcal{W}_c , which are the coefficient matrices $\mathbf{F}_c, \mathbf{g}_c$ in Equation (5).

Refer to Section II-B for a discussion on transforming between the two representations (H and V) of a polytope. A more detail application of this technique applied in the context of legged locomotion can be found in [8].

D. Approximating the grasp stability constraint

In practice, \mathbf{F}_c might have many rows, causing computational difficulties during motion planning. We alleviate this issue by approximating the set of physically realizable

⁵There can not be generating rays since $\hat{\mathcal{F}}$ is bounded.

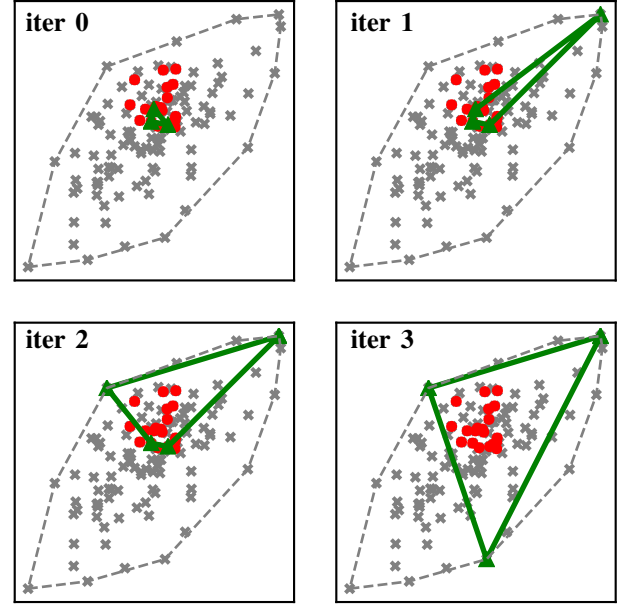


Fig. 4. Application of the proposed procedure for approximating grasp stability constraint on a planar data set. Vertices $\hat{\mathbf{w}}_i$ are shown as gray crosses; guiding samples are shown as red dots. The proposed procedure finds 3 vertices (iter 3) whose convex hull covers the guiding samples completely. In comparison, the dashed grey polygon, representing the exact constraint, has four times as many edges.

wrenches as the convex hull of a *set* of points \mathcal{Y} that (i) is a subset of \mathcal{W}_c and (ii) contains interacting wrenches that are *the most likely to be realized during execution*. To achieve the latter objective, we randomly sample potentially interacting wrenches, referred to as *guiding samples*. This can be done offline by generating a few random trajectories in the same workspace, sample a number of points in each trajectory, and for each point compute the interacting wrench using the Newton-Euler equations. Subsequently, we extend \mathcal{Y} from a simple initial guess to cover more guiding samples in an iterative fashion.

Concretely, the procedure proceeds as follows:

- 1) randomly sample N guiding samples; only samples that belongs to \mathcal{W}_c are retained;
- 2) initialize \mathcal{Y} as a simplex with 7 randomly chosen guiding samples as vertices;
- 3) compute the convex hull \mathcal{H} of \mathcal{Y} ;
- 4) choose the face h^* of \mathcal{H} that contains the most guiding samples in its infeasible halfspace;
- 5) add to \mathcal{Y} the vertex in \mathcal{W}_c that is in the infeasible halfspace of h^* and is furthest away from it;
- 6) repeat from step 3 until the number of vertices in \mathcal{Y} is greater than a specified value.

Remark that in step 2 since the wrench space is 6 dimensional, a simplex in this space has 7 vertices. Hence, this step amounts to choosing randomly 7 guiding samples. After each iteration, a point in $(\hat{\mathbf{w}}_1, \dots, \hat{\mathbf{w}}_l) \setminus \mathcal{Y}$ is added to \mathcal{Y} . We found that after about 50 iteration, the convex hull of \mathcal{Y} covers

a significant portion of the guiding samples and contains approximately 3000-4000 faces. In contrast, the original H-representation can have up to 150000 faces.

An application of this procedure on a planar data set is demonstrated in Fig. 4. There, the green triangle representing the approximate grasp constraint that has only 3 edges but cover all guiding samples. This result is computed in 3 extending iterations. In comparison, the dashed grey polygon, representing the exact constraint, has four times as many edges.

III. PLANNING CRITICALLY FAST MOVEMENTS

A. Motion planning pipeline

We implement a pipeline for planning critically fast movements following the *decoupling approach*:

- 1) Find a collision-free path using standard geometric planners (e.g. RRT [9]);
- 2) Time-parameterize the collision-free path to minimize traversal time under kinodynamic constraints (in our case: joint velocity and acceleration bounds and suction cup constraints).

Although the decoupling approach does not generally produce optimal nor even locally-optimal trajectories, it has the distinctive advantage of being robust and fast. This is due to the highly mature states of collision-free path planning and path time-parameterization techniques [10].

Regarding the latter, the problem of finding the time-optimal time-parameterization of a geometric path subject to kinodynamic constraints is a classical problem in robotics [11]. If the constraints under consideration are of First- or Second-Order (see below and also in [12]), then this problem can be solved extremely efficiently using the recently-developed Time-Optimal Path Parameterization via Reachability Analysis (TOPP-RA) algorithm [12].

In the next section, we show that the grasp stability constraint is a Second-Order constraint.

B. Reduction of the grasp stability constraint

A Second-Order constraint has the following form [12]

$$\mathbf{A}(\mathbf{q})\ddot{\mathbf{q}} + \dot{\mathbf{q}}^\top \mathbf{B}(\mathbf{q})\dot{\mathbf{q}} + \mathbf{f}(\mathbf{q}) \in \mathcal{C}(\mathbf{q}), \quad (6)$$

- $\mathbf{A}, \mathbf{B}, \mathbf{f}$ are continuous mappings from \mathbb{R}^n to $\mathbb{R}^{m \times n}$, $\mathbb{R}^{n \times m \times n}$ and \mathbb{R}^m respectively;
- $\mathcal{C}(\mathbf{q})$ is a convex polytope in \mathbb{R}^m .

To establish that any grasp stability constraint can be reformulated as a Second-Order constraint, recall first the following relationships between the robot's joint position and the object's motion [13]:

$$\boldsymbol{\omega}_b = \mathbf{J}_{\text{rot}}(\mathbf{q})\dot{\mathbf{q}}, \quad \boldsymbol{\alpha}_b = \mathbf{J}_{\text{rot}}(\mathbf{q})\ddot{\mathbf{q}} + \dot{\mathbf{q}}^\top \mathbf{H}_{\text{rot}}(\mathbf{q})\dot{\mathbf{q}}, \quad (7)$$

$$\mathbf{v}_b = \mathbf{J}_{\text{trans}}(\mathbf{q})\dot{\mathbf{q}}, \quad \mathbf{a}_b = \mathbf{J}_{\text{trans}}(\mathbf{q})\ddot{\mathbf{q}} + \dot{\mathbf{q}}^\top \mathbf{H}_{\text{trans}}(\mathbf{q})\dot{\mathbf{q}}, \quad (8)$$

where $\mathbf{J}_\square, \mathbf{H}_\square$ are the translational and rotational Jacobians and Hessians, $\mathbf{v}_b, \boldsymbol{\omega}_b$ denote the object's translational and rotational velocities and $\mathbf{a}_b, \boldsymbol{\alpha}_b$ denote the translational and rotational accelerations; all are in the object's body frame

$\{b\}$. Next, combining Equations (7) and (8) with the Newton and Newton-Euler equations in the body frame, which are

$$\mathbf{w}_b + \begin{bmatrix} 0_3 \\ \mathbf{g}_b m \end{bmatrix} = \begin{bmatrix} \mathbf{I}_b \boldsymbol{\alpha}_b + \boldsymbol{\omega}_b \times \mathbf{I}_b \boldsymbol{\omega}_b \\ m \mathbf{a}_b \end{bmatrix}. \quad (9)$$

It follows that the interaction wrench in frame $\{b\}$ has the following form

$$\mathbf{w}_b(\mathbf{q}, \dot{\mathbf{q}}, \ddot{\mathbf{q}}) = \Theta_1(\mathbf{q})\ddot{\mathbf{q}} + \dot{\mathbf{q}}^\top \Theta_2(\mathbf{q})\dot{\mathbf{q}} + \Theta_3(\mathbf{q}),$$

where $\Theta_1, \Theta_2, \Theta_3$ are tensors depending on the geometry of the robot and the inertial properties of the object. The left hand-side shows clearly that \mathbf{w}_b also depends on $\mathbf{q}, \dot{\mathbf{q}}, \ddot{\mathbf{q}}$.

Next, let \mathbf{G}_{cb} be the *constant* matrix that transforms a wrench from the object's body frame $\{b\}$ to the suction cup's frame $\{c\}$. Substituting to Equation (5), grasp stability constraint can then be written as

$$\mathbf{F}_c \mathbf{G}_{cb} \{ \Theta_1(\mathbf{q})\ddot{\mathbf{q}} + \dot{\mathbf{q}}^\top \Theta_2(\mathbf{q})\dot{\mathbf{q}} + \Theta_3(\mathbf{q}) \} \leq \mathbf{g}_c. \quad (10)$$

It follows immediately that Equation (10) is a Second-Order constraint. Indeed, $\Theta_1, \Theta_2, \Theta_3$ take the place of $\mathbf{A}, \mathbf{B}, \mathbf{f}$ respectively and the fixed convex polytope

$$\{ \mathbf{w}_b \mid \mathbf{F}_c \mathbf{G}_{cb} \mathbf{w}_b \leq \mathbf{g}_c \}.$$

takes the place of $\mathcal{C}(\mathbf{q})$.

IV. EXPERIMENTS

Two aspects of the proposed approach were experimentally investigated. First, we evaluate the *quality* of the trajectories for transporting object by looking at the rate of successful transport and the trajectories' durations in 20 randomly generated instances (IV-A). Second, we report the actual computational cost of the proposed pipeline in a realistic pick-and-place scenario (IV-B).

A. Experimental setup

The same equipment was employed throughout the experiments. These include a position-controlled industrial robot Denso VS-060, equipped with a suction cup connected to a vacuum pump. The robot is controlled at 125 Hz. The suction cup has a radius of 12.5 mm and the vacuum pump generates a negative pressure of approximately 30 kPa. Objects considered in the experiments have varying weights ranging from 0.2 kg to 0.6 kg; all objects have known weights and moment of inertia. All computations were done on a single core of a laptop running Ubuntu 16.04 at 3.800 GHz.

Collision-free paths between two robot configurations were all computed using OpenRAVE's implementation [14] of `birrt` algorithm [9].

For time-parameterization, we used the same approximation of the grasp stability constraint in all experiments. The coefficients matrices $\mathbf{F}_c, \mathbf{g}_c$ were identified following the procedure given in Section II with the following parameters: $m = 6$ points are used to approximate the surface area contact; coefficient of friction $\mu = 0.3$ (identified in prior using a Force-Torque sensor); suction cup radius is 12.5 mm; maximum number of vertices is 60. The resulting coefficient matrices have 3099 rows, which is significantly

less than the number of rows of the exact coefficient matrices (130000 rows). All TOPP instances are discretized with 100 gridpoints, using the first-order interpolation scheme [12]. The code is written mostly in Python, with the most computationally demanding components written in Cython and C++. TOPP-RA solves the LPs using a custom LP solver based on Seidel’s algorithm [15].

B. Trajectory quality

We first looked at the likelihood of the objects falling, slipping or twisting when executing the trajectories found by our pipeline. As a baseline for comparison, we also considered an alternative strategy, where one computes time-optimal time-parameterizations subject only to the robot’s kinematic constraints, without taking into account the suction cup constraint.

Twenty geometric paths were randomly generated and tested. To mimic actual pick-and-place settings, we adopted the following procedure:

- 1) sample randomly the object’s starting and goal poses, each in a dedicated region of the workspace;
- 2) use OpenRAVE’s inverse kinematics to find the corresponding robot’s starting and goal configurations;
- 3) find a path between the starting and goal configurations using OpenRAVE.

In all trials, a rectangle notebook (See Fig. 5) with weight 0.551 kg and moment of inertia $\text{diag}(9.28, 21.10, 29.80) \times 10^{-4} \text{ kgm}^2$ was transported with the suction cup. The contact point is 12.5 mm above the notebook’s center of mass.

It was found that, by considering grasp stability, the object could be transported without slipping or falling for all 20 paths (Table I). On the other hand, trajectories retimed without suction cup constraint had a much lower success rate: only 4 out of 20 paths could be executed successfully. Remarkably, trajectories computed considering grasp stability were not significantly slower. For example, slowing respectively trajectory number 2 by 6.3% and trajectory 14 by 20% made those trajectories safe.

A second experiment was performed to examine the degree of sub-optimality. We took paths number 12 and 18, parameterized both subject to grasp stability constraint and executed them at three levels of speed: 100%, 120%, 140%. We then inspected the pose of the object relative to the suction cup after each execution. Significant slipping of nearly 1 cm and 10 deg were found at the trials executed at 120% and 140% speed, see Fig. 5 and first part of the experimental video <https://youtu.be/b9H-zOYWlBY>.

C. Computational performance

To investigate the computational cost of the proposed approach, we considered a pick-and-place scenario that involves the robot picking objects using the suction cup from a bin and stacking them at a distant goal position (Fig. 1). The objective is to complete the task as fast as possible, planning and execution time included. The object properties, initial poses and final desired poses were determined prior

TABLE I
TRAJECTORY DURATION (IN SECONDS) AND SUCCESS RATE OF 20 RANDOMLY GENERATED TRAJECTORIES RETIMED WITHOUT AND WITH SUCTION CUP CONSTRAINTS (SCC).

#	without SCC	with SCC	time ext. (%)
0	0.432 ✗	0.672 ✓	35.71
1	0.568 ✗	0.832 ✓	31.73
2	0.944 ✗	1.008 ✓	6.35
3	0.504 ✗	0.688 ✓	26.74
4	0.728 ✗	0.952 ✓	23.53
5	0.504 ✗	0.672 ✓	25.00
6	1.064 ✓	1.064 ✓	0.00
7	0.520 ✗	0.688 ✓	24.42
8	1.136 ✗	1.344 ✓	15.48
9	0.496 ✗	0.744 ✓	33.33
10	0.632 ✓	0.728 ✓	13.19
11	0.520 ✗	0.648 ✓	19.75
12	0.440 ✗	0.728 ✓	39.56
13	0.824 ✓	0.896 ✓	8.04
14	1.104 ✗	1.392 ✓	20.69
15	0.528 ✗	0.664 ✓	20.48
16	0.520 ✗	0.736 ✓	29.35
17	1.344 ✗	1.848 ✓	27.27
18	0.472 ✗	0.760 ✓	37.89
19	0.512 ✓	0.600 ✓	14.67

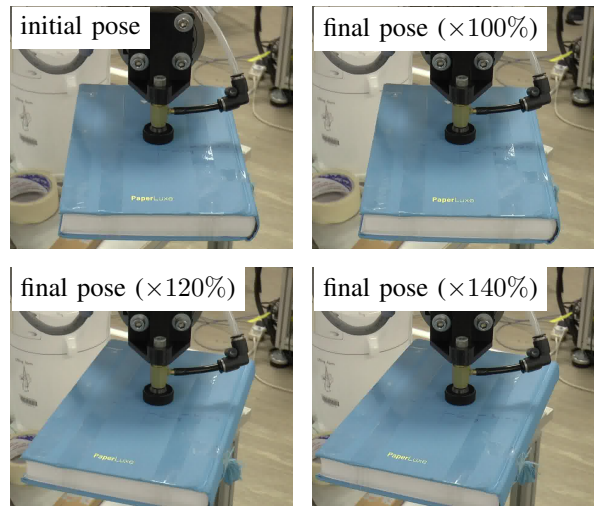


Fig. 5. Executing a retimed trajectory at 120% and 140% speed led to visible twisting and slipping.

TABLE II
BREAKDOWN OF CYCLE TIMES (IN SECONDS)

	obj 1	obj 2	obj 3	obj 4
APPROACH plan	0.018	0.053	0.016	0.041
REACH plan	0.029	0.034	0.040	0.034
MOVE plan	0.183	0.101	0.147	0.198
MOVE retime	0.111	0.111	0.124	0.137
Total plan	0.341	0.299	0.327	0.410
APPROACH exec.	0.438	0.747	0.550	0.531
REACH exec.	0.306	0.368	0.415	0.436
ATTACH delay	1	1	1	1
MOVE exec.	0.841	0.729	1.062	1.371
DETACH delay	1	1	1	1
Total exec.	3.585	3.844	4.027	4.338
Total (plan + exec.)	3.926	4.143	4.354	4.748

to the experiment. The objects weighted between 0.204 kg and 0.551 kg.

A pick-and-place cycle consisted of several phases. First, the robot *approaches* a pose that is directly on top of the bin. Then, it *reaches* for the topmost object, closes the vacuum valve, waits for 1 second for the object to *attach* to the suction cup, and finally *moves* to the given destination. When the robot arrives at the destination, it opens the valve and waits for 1 second for the object to completely *detach* before starting the next cycle. Note that the waiting times of 1 second could be reduced.

All collision-free paths were planned *online* using OpenRAVE. Time-parameterization was also performed *online* subject to the grasp stability constraint in addition to the robot’s kinematic limits.

The experiment can be visualized in the second part of the experimental video. Table II reports our findings. Pick-and-place cycles were less than 5 sec for all objects. On average, the cycle time was 4.29 sec, of which 0.34 sec was for trajectory planning (including path planning and time-parameterization), 1.95 sec was for robot motion, and 2 sec was for waiting for the pump.

V. RELATED WORKS

Several researchers have investigated a closely related problem: the “waiter problem”. In this problem, a robot, equipped with a flat plate, is tasked with transporting an object that is *only placed* on the plate. A popular approach that was taken in [16], [17], [18] is to enforce grasp stability constraint by constraining the Zero-tilting Moment Point [19] (ZMP) of the object to its support area. This elegant idea demonstrates the common points between object transportation and humanoid locomotion but, at the same time, brings with it two limitations of the classical ZMP concept: it requires the object to stay on a flat surface and is unable to prevent the object from slipping and twisting [20]. In a more recent work [21], Luo and Hauser proposes to consider the *individual* contact forces explicitly, eliminating the use of the ZMP and its limitations. However, their formulation leads to a non-convex non-linear optimization problem that is computationally demanding, taking several seconds to terminate.

In contrast, our approach utilizes polyhedral computational theory to obtain a much more concise problem formulation, which can be solved significantly faster. This approach is inspired by another development in humanoid locomotion: the use of the Gravitational-Inertia Wrench Cone to guarantee contact stability [8], [7].

All prior works in the literature formulate and solve a form of the Time-Optimal Path Parameterization (TOPP) to obtain the final motion. TOPP is a classic problem in robotics: since the pioneering work [11], there have been several notable developments. Verschuere showed that TOPP with Second-Order constraints is a convex optimization problem [22] and proposed several algorithmic solutions. Hauser proposed a more efficient Sequential Linear Programming

algorithm [23]. Singular switch points were then characterized, on which a robust implementation of the Numerical Integration-based algorithm of Bobrow for solving TOPP was developed [24]. Recently, we have introduced TOPP-RA, a new algorithm to solve TOPP that is also the algorithm utilized in this work [12]. A more detailed review of the literature can be found in [12].

Several groups have reported on the development of *complete* robotic pick-and-place systems [25], [26]. These reports offer a broader view of pick-and-place system and are more focused on the perception/vision sub-module. Regarding motion planning, these works often employ reactive strategies that are based on online visual feedback. In contrast, our approach fits entirely in the more conventional sense-plan-act strategy. It is clear that with sufficient knowledge of the external environment, the proposed approach offers a much higher level of performance. However, it remains to be seen how the approaches compete in relatively uncertain environment.

VI. CONCLUSION

We have proposed an approach for planning critically fast trajectories for manipulators performing pick-and-place with suction cup. Before execution, we identify the grasp stability constraint, the constraint that the object must not fall from or slip or twist relatively to the suction cup, as a system of linear inequalities. During execution, we plan collision-free geometric paths for transporting objects and retune these paths *time-optimally* subject to the identified grasp stability constraint using the TOPP-RA algorithm.

Experiments were conducted to assess the performance of the proposed approach. The results suggest that the approach is capable of producing high-quality trajectories: these trajectories can be executed successfully without causing the object to fall or slip and have duration that were close to the true time-optimal values. Further, we also found that the proposed approach has a low computational cost, making it suitable for online motion planning for logistics applications.

There are two limitations that we are actively investigating:

- Our approach requires exact knowledge of the object’s inertial properties: center-of-mass position, mass and moment of inertia and the robot’s geometry. Yet, in a practical setting, identification and modelling errors always exist. Usually, only approximations of objects’ properties are available. This observation leads to two questions: 1) what are the effects of identification errors on motion quality and 2) how to handle these errors;
- The approximation step presented in Section II-D reduces computational time significantly as the size of the grasp stability constraint is much smaller. However, its effects on motion quality is, in general, not completely understood.

Acknowledgment

This work was partially supported by the Medium-Sized Centre funding scheme (awarded by the National Research Foundation, Prime Minister’s Office, Singapore).

REFERENCES

- [1] J.-S. Pang and J. Trinkle, "Stability characterizations of rigid body contact problems with coulomb friction," *ZAMM-Journal of Applied Mathematics and Mechanics/Zeitschrift für Angewandte Mathematik und Mechanik*, vol. 80, no. 10, pp. 643–663, 2000.
- [2] S. Caron, Q.-C. Pham, and Y. Nakamura, "Stability of surface contacts for humanoid robots: Closed-form formulae of the contact wrench cone for rectangular support areas," in *2015 IEEE International Conference on Robotics and Automation (ICRA)*. IEEE, 2015, pp. 5107–5112.
- [3] S. Boyd and L. Vandenberghe, *Convex Optimization*. New York, NY, USA: Cambridge University Press, 2004.
- [4] a. Ben-Tal and a. Nemirovski, "On Polyhedral Approximations of the Second-Order Cone," *Mathematics of Operations Research*, 2001.
- [5] K. Fukuda and A. Prodon, "Double description method revisited," in *Combinatorics and computer science*. Springer, 1996, pp. 91–111.
- [6] D. Avis and K. Fukuda, "Reverse search for enumeration," *Discrete Applied Mathematics*, 1996.
- [7] S. Caron, Q.-C. Pham, and Y. Nakamura, "ZMP Support Areas for Multicontact Mobility Under Frictional Constraints," *IEEE Transactions on Robotics*, vol. 33, no. 1, pp. 67–80, feb 2017.
- [8] —, "Leveraging cone double description for multi-contact stability of humanoids with applications to statics and dynamics," *Robotics: Science and System*, 2015.
- [9] J. J. Kuffner and S. M. LaValle, "RRT-connect: An efficient approach to single-query path planning," in *Robotics and Automation, 2000. Proceedings. ICRA'00. IEEE International Conference on*, vol. 2. IEEE, 2000, pp. 995–1001.
- [10] Q.-C. Pham, S. Caron, P. Lertkultanon, and Y. Nakamura, "Admissible velocity propagation: Beyond quasi-static path planning for high-dimensional robots," *The International Journal of Robotics Research*, vol. 36, no. 1, pp. 44–67, 2017.
- [11] J. E. Bobrow, S. Dubowsky, and J. S. Gibson, "Time-optimal control of robotic manipulators along specified paths," *The international journal of robotics research*, vol. 4, no. 3, pp. 3–17, 1985.
- [12] H. Pham and Q. C. Pham, "A New Approach to Time-Optimal Path Parameterization Based on Reachability Analysis," *IEEE Transactions on Robotics*, vol. 34, no. 3, pp. 645–659, 2018. [Online]. Available: <https://arxiv.org/abs/1707.07239>
- [13] a. Hourtash, "The Kinematic Hessian and Higher Derivatives," *2005 International Symposium on Computational Intelligence in Robotics and Automation*, 2005.
- [14] R. Diankov and J. Kuffner, "OpenRAVE : A Planning Architecture for Autonomous Robotics," *Robotics*, no. July, pp. –34, 2008. [Online]. Available: http://www.ri.cmu.edu/pub_files/pub4/diankov_rosen.2008.2/diankov_rosen.2008.2.pdf
- [15] R. Seidel, "Small-dimensional linear programming and convex hulls made easy," *Discrete & Computational Geometry*, vol. 6, no. 3, pp. 423–434, 1991.
- [16] P. Lertkultanon and Q. C. Pham, "Dynamic non-prehensile object transportation," in *2014 13th International Conference on Control Automation Robotics and Vision, ICARCV 2014*. IEEE, 2014, pp. 1392–1397.
- [17] F. G. Flores and A. Kecskeméthy, "Time-optimal path planning for the general waiter motion problem," in *Mechanisms and Machine Science*, V. Kumar, J. Schmiedeler, S. V. Sreenivasan, and H.-J. Su, Eds. Heidelberg: Springer International Publishing, 2013, vol. 14, pp. 189–203. [Online]. Available: https://doi.org/10.1007/978-3-319-00398-6_14
- [18] G. Csorvási, Á. Nagy, and I. Vajk, "Near Time-Optimal Path Tracking Method for Waiter Motion Problem," *IFAC-PapersOnLine*, vol. 50, no. 1, pp. 4929–4934, 2017.
- [19] M. Vukobratović and B. Borovac, "Zero-Moment Point Thirty Five Years of Its Life," *International Journal of Humanoid Robotics*, vol. 01, no. 01, pp. 157–173, 2004.
- [20] P. Sardain and G. Bessonnet, "Forces acting on a biped robot. Center of pressure-zero moment point," *IEEE Transactions on Systems, Man, and Cybernetics-Part A: Systems and Humans*, vol. 34, no. 5, pp. 630–637, 2004.
- [21] J. Luo and K. Hauser, "Robust trajectory optimization under frictional contact with iterative learning," *Autonomous Robots*, vol. 41, no. 6, pp. 1447–1461, 2017.
- [22] D. Verscheure, B. Demeulenaere, J. Swevers, J. De Schutter, and M. Diehl, "Practical time-optimal trajectory planning for robots: a convex optimization approach," *IEEE Transactions on Automatic Control*, 2008.
- [23] K. Hauser, "Fast interpolation and time-optimization with contact," *The International Journal of Robotics Research*, vol. 33, no. 9, pp. 1231–1250, aug 2014.
- [24] Q.-C. Pham, "A General, Fast, and Robust Implementation of the Time-Optimal Path Parameterization Algorithm," *IEEE Transactions on Robotics*, vol. 30, no. 6, pp. 1533–1540, dec 2014.
- [25] N. Correll, K. E. Bekris, D. Berenson, O. Brock, A. Causo, K. Hauser, K. Okada, A. Rodriguez, J. M. Romano, and P. R. Wurman, "Analysis and Observations from the First Amazon Picking Challenge," *IEEE Transactions on Automation Science and Engineering*, 2016. [Online]. Available: <http://arxiv.org/abs/1601.05484>
- [26] D. Morrison, A. W. Tow, M. McTaggart, R. Smith, N. Kelly-Boxall, S. Wade-McCue, J. Erskine, R. Grinover, A. Gurman, and T. Hunn, "Cartman: The low-cost cartesian manipulator that won the amazon robotics challenge," *arXiv preprint arXiv:1709.06283*, 2017.